A hybrid multiple sensor fault detection, diagnosis and reconstruction algorithm for chiller plants

K. F. Fong [1]*, C. K. Lee [1], M. K. H. Leung [2], Y. J. Sun [1], Guangya Zhu [3], Seung Hyo Baek [4], X. J. Luo [5], Tim Ka Kui Lo [6], Hetty Sin Ying Leung [6]

* Corresponding author, Email: bssquare@cityu.edu.hk; Tel: (852) 3442 8724; Fax: (852) 3442 9716

1 Division of Building Science and Technology, College of Engineering, City University of Hong Kong

2 School of Energy and Environment, City University of Hong Kong

3 College of Aerospace Engineering, Nanjing University of Aeronautics and Astronautics

4 Division of Architecture, Mokwon University

5 Department of Accounting, Economics and Finance, Faculty of Business and Law, University of the West of England

6 Smart Infrastructure, Siemens Limited

Abstract

In a chiller plant, primary or critical sensors are used to control the system operation while secondary sensors are installed to monitor the performance/health of individual equipment. Current sensor fault detection and diagnosis (SFDD) approaches are not applicable to secondary sensors which usually are not involved in the system control. Consequently, a hybrid multiple sensor fault detection, diagnosis and reconstruction (HMSFDDR) algorithm for chiller plants was developed. Machine learning and pattern recognition were used to predict the primary sensor faults through the comparison of the weekly performance curves. With the primary sensors signals reconstructed, the secondary sensor faults were estimated based on mass and energy balance. By applying the algorithm with various logged plant data and comparison with site checking results, a maximum of 75% effectiveness could be achieved. The merits of the present approach were further justified through off-site sensor testing which reinforced the usefulness of proposed HMSFDDR algorithm.

Keywords

Fault detection and diagnosis; big data analytics; machine learning; pattern recognition; chiller plant; sensor faults.

1. Introduction

Digitalization in HVAC systems is getting popular nowadays. By the proper analysis on past performance data and issue trends through fault detection and diagnosis (FDD), abnormal or faulty control and energy saving opportunities may be identified through simulation and predictive technologies. Studies on FDD of air-conditioning systems have been made in recent decades. The applied methods for FDD can be mainly divided into three categories according to the system modeling approach, namely quantitative model-based, qualitative model-based and process history-based according to Venkatasubramanian *et al.* (2003a~c). According to Kim and Katipamula (2018), over 60% of the published FDD studies adopted the process history-based approach particularly using statistical black box methods.

In the chiller plant, reliable and accurate sensor measurements are essential for monitoring the system/equipment performance, implementing control strategies and diagnosing equipment and system performance. Primary or critical sensors (CS) are used in the system control while secondary sensors (SS) were employed to indicate the performance/health of individual equipment. Since different kinds of sensor faults may occur in the chiller plant, sensor fault detection and diagnosis (SFDD) is useful and somehow critical to ensure the proper system operation. In particular, sensor fault reconstruction is sometimes essential as it may not be convenient to replace a faulty sensor immediately in actual practice.

Numbers of studies have been made on SFDD of chiller plants using the process history-based approach. Wang *et al.* (2001) devised a method for the SFDD of chiller system based on a normalized energy balance residual approach. Wang and Cui (2005) applied PCA method to diagnose and reconstruct sensor faults in centrifugal chiller systems. Sun *et al.* (2010) presented a sensor fault diagnosis method for a chiller plant which employed a data fusion algorithm to diagnose the faults when calculating the system cooling load through direct measurement. Wang *et al.* (2010) proposed a FDD strategy which involved system and sensor faults for HVAC systems. They remarked that SFDD with reconstruction could still work well under different system fault situations. Li *et al.*

(2016) applied the support vector data description (SVDD) algorithm to conduct SFDD of a screw chiller system. They compared the SFDD effectiveness with that based on the PCA and found that the proposed method offered similar performance in fault detection but better results in fault diagnosis under various fault conditions.

Wang *et al.* (2018) presented a decentralized SFDD method with reconstruction for HVAC systems by employing an exponential function to diagnose and reconstruct the sensor readings. Gao *et al.* (2019) devised a SFDD algorithm by using virtual sensors which were highly correlated to different groups of actual sensors in an air-conditioning system. Zhang *et al.* (2019) proposed a SFDD approach based on PCA and clustering method with the combined k-means and subtractive clustering employed to identify and classify modeling data in unsteady operating conditions. Luo *et al.* (2019) developed a SFDD strategy by employing k-means clustering for a chilled water system. With system operation data simulated by using TRNSYS, a total centroid score profile was established for four typical weeks throughout a year to detect and diagnose the various sensor faults. Elnour *et al.* (2020) presented a SFDD method based on auto-associative neural network (AANN). They found that data validation and diagnostic accuracy was improved as compared to that based on the PCA. However, their method could not reconstruct the sensor signal. Ng *et al.* (2020) employed the Bayesian method to predict the temperature and flow sensor faults in a chiller plant with ideal sensor arrangement. Wu *et al.* (2021) applied the partial least square method to diagnose the sensor fault in a chiller plant. They claimed that the results were better than those using the PCA method.

Through the above literature review, studies on SFDD using big data analytics were mainly focused on primary or critical sensors which were used in the system control. For secondary sensors, the employed approaches are generally not effective. Moreover, secondary sensors can be correlated to the system performance only when the associated equipment is in operation. For example, when any chiller is not running, there will be no water flow past that chiller according to the common design practice. In this regard, the water temperatures at both ends of the chiller can be quite different from those of the critical ones even if the secondary temperature sensors are still healthy. If the same approach is to be used for both types of sensors, then only those operating data in which all the major equipment are in operation can be used. This may only occur during the peak-load period, and SFDD cannot be conducted outside the peak-load period.

To solve the problem, it is evident that a different approach should be used in order to perform SFDD for the secondary sensors. Hence, it was the intent of this paper to derive an algorithm to diagnose and reconstruct both primary and secondary sensor faults in a chilled water system which combined big data analytics and thermodynamics. Actual logged system operation data and site checking reports from various plants were used to justify the effectiveness of the algorithm. Besides, a comprehensive data refinement procedure was introduced to better the quality of the input data for system modeling and fault evaluation rather than just screening out the suspected data set.

2. Algorithm development

2.1 Research methodology and outline of algorithm

Figure 1 depicts the symbolic diagram of a centralized water-cooled chilled water system which indicates the locations of the various CS and SS considered. It was evident that all critical sensors were correlated to the chiller plant performance whenever the plant was in operation but not necessarily for all the secondary sensors. The SS were not included in the plant control. Their readings were coupled with the plant operation only when the associated equipment was running as indicated in Figure 1.

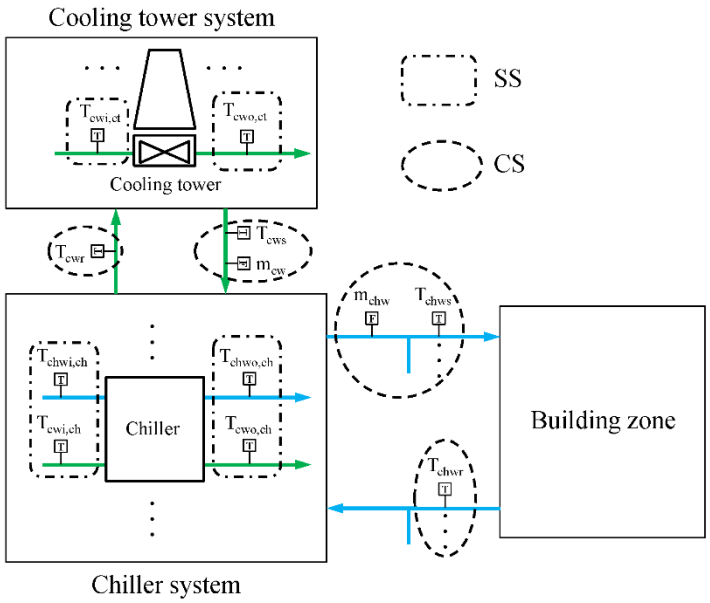

Figure 1. Symbolic diagram of a centralized water-cooled chilled water system.

In this study, a hybrid multiple sensor fault detection, diagnosis and reconstruction (HMSFDDR) algorithm [with a patent application filed (Lo *et al.* 2022)] was developed and executed to determine any potential sensor fault signals from both CS and SS. For CS, it was based on machine learning and pattern recognition. For SS, their readings might not be closely coupled to the chiller plant performance throughout the entire operating schedule. Hence, the analysis method was different from those for the critical sensors. Instead, thermodynamics approach was employed. The open-source Python programming platform was employed to build the HMSFDDR algorithm due to its familiarity in artificial intelligence and machine-learning studies. Many downloadable plugins are available which are commonly used in pattern recognition like ANN modeling and k-means clustering. Figure 2, shows the outline of the HMSFDDR algorithm. Detailed description would be given in Section 2.2.

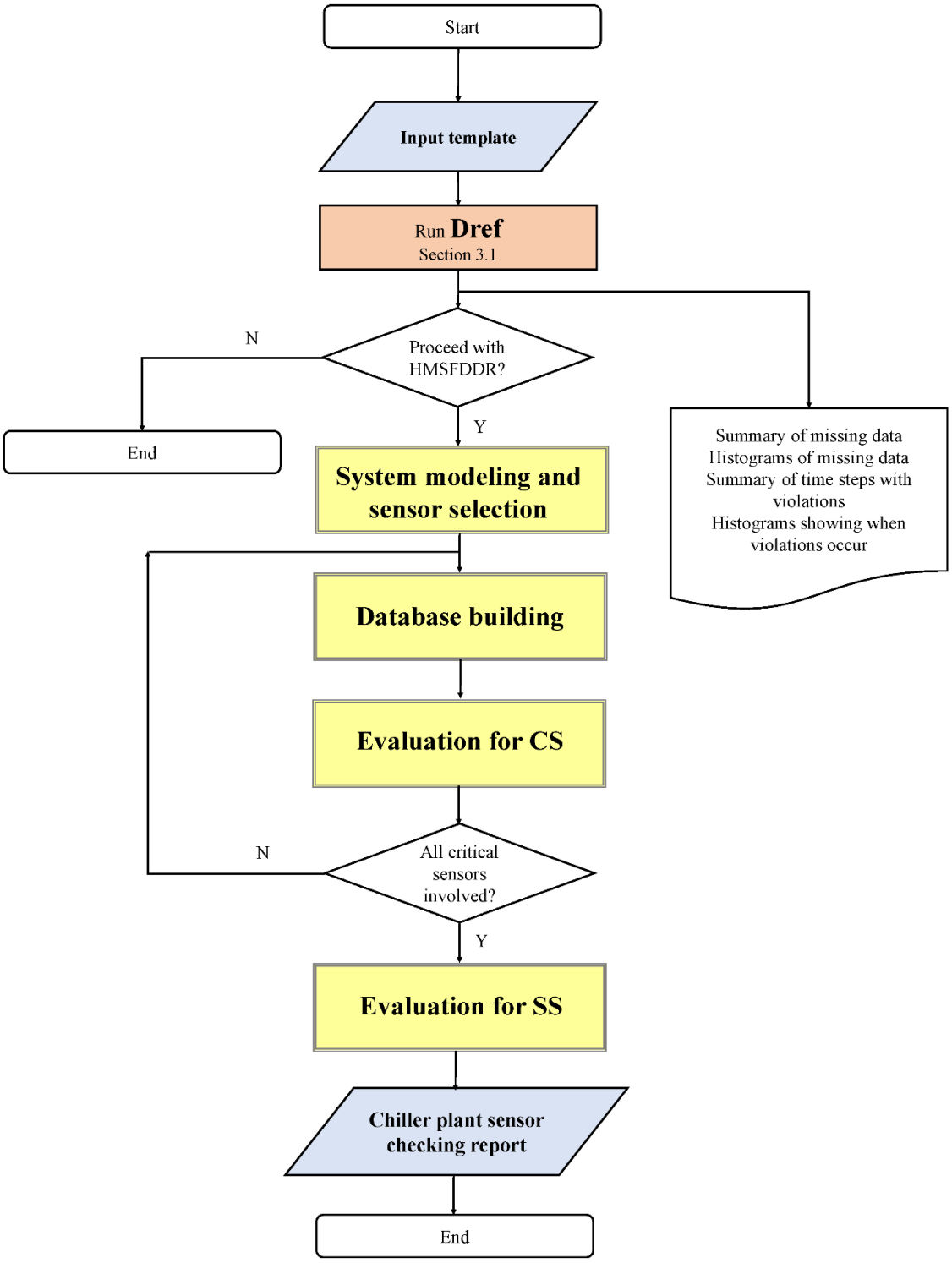

Figure 2. Overall flowchart for the HMSFDDR algorithm.

2.2. Detailed description of algorithm

According to Figure 2, the HMSFDDR comprised various processes, namely **system modeling and sensor selection**, **database building**, **evaluation for CS** and

evaluation for SS. Different subroutines were involved, namely data refinement (DRef), system modeling (SMod), sensor selection (SSel) for CS, sensor fault detection (SFDet) for CS, sensor fault diagnosis (SFDia) for CS, sensor fault reconstruction (SFRec) for CS and fault evaluation of SS as detailed in the following sub-sections. Before performing the HMSFDDR, it might be useful and necessary to pre-screen the quality of the logged data first in order to determine whether it could be used for HMSFDDR. Hence, the programme allowed if only a quality check of the input data was to be done. In this way, only the DRef subroutine was executed. Users could then determine if HMSFDDR should be continued.

Figure 3 shows the detailed description of the HMSFDDR algorithm. During the execution of HMSFDDR, information transfer across the different processes was needed through data files as indicated by Ⓐ to Ⓖ in Figure 3.

In **system modeling and sensor selection**, three input datasets would be generated for system modeling, fault evaluation of CS (Ⓐ) and SS (Ⓑ) respectively. Then, the ANN system model was established by using the SMod subroutine, followed by the SSel subroutine to determine if all the critical sensors should be involved. The normalized dataset used for SMod (Ⓒ) as well as the parameters of the ANN model (Ⓓ) were stored for later use.

In **database building**, the databases for the fault-free and faulty centroid scores of the considered critical sensors were built in the SFDet and SFDia (for database building) subroutines for use in the fault evaluation of CS as shown in Figure 3. The normalized dataset used for SMod (Ⓒ) as well as the parameters of the ANN model (Ⓓ) were read in order to determine the respective fault-free (Ⓔ) and faulty (Ⓕ) centroid score database.

In **evaluation for CS**, the input dataset (Ⓐ) and the fault-free centroid score database (Ⓔ) were used generate the evaluation centroid score database in SFDet (for evaluation). Then, the respective faults for the critical sensors were determined in SFDia (for evaluation) and the fault reconstruction database (Ⓖ) generated in SFRec.

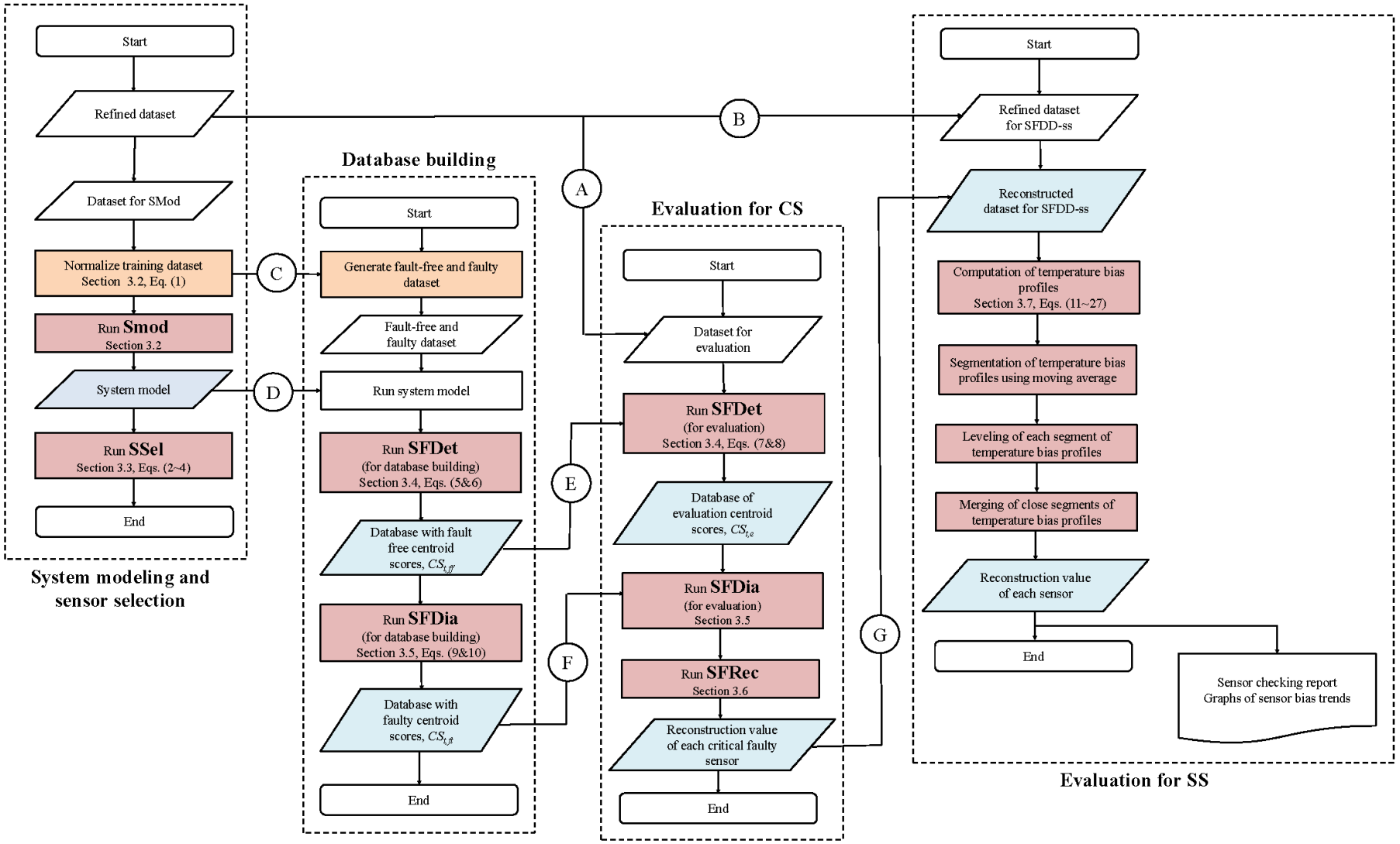

Figure 3. Detailed description of the HMSFDDR algorithm.

In **evaluation for SS**, the input dataset (Ⓑ) and the fault reconstruction database (Ⓖ) were used to compute the temperature bias profile of each secondary sensor.

2.2.1 Data refinement

The logged data from the BMS system at different sites may have different formats and structures for the same signals. Sometimes, the logged information is incomplete with missing data at particular time steps and/or signals. To worsen the situation, some logged data may not be within the reasonable range, say a negative value for equipment power, and that some logged data may appear to be in conflict such as a recorded equipment power when the equipment status is OFF. Consequently, a data refinement procedure is necessary which has two purposes. The first one is to check the quality of the logged data. This is useful as some information may be collected regarding the health of the sensors through this process. The second purpose is that a reasonable logged data is important for building the system model (further elaborated in the Section 2.2.2).

The data refinement steps can be grouped into four categories, namely conversion of non-numeric data to numeric (R0), check for missing data (R1), check for data out-of-range (R2) and check for data conflict with equipment on/off status (R3) as summarized in Appendix B. Upon completion of the data refinement subroutine, various data files would be created which recorded the data refinement checking results. In the complete HMSFDDR algorithm, three datasets are required as already mentioned before. The time-dependent input data was divided into two parts. The first part was used for modeling training and database building while the latter one was used for fault evaluation of critical sensors. The ratio of the training period was governed by the training period ratio ($Train_{ratio}$) as specified in the time-independent input template. As the model training, database building and fault evaluation of critical sensors did not require secondary sensor signals (except the chilled water supply temperature), less information was needed. Meanwhile, the dataset for the fault evaluation of secondary sensors involved all the data points within the evaluation period.

2.2.2 System modeling

To investigate the performance of the system under a faulty signal, a proper system model should be developed. For a chiller plant, various design configurations may be adopted which include water-cooled system, air-cooled system, primary chilled water pipe system, primary and secondary chilled water pipe system, constant-speed pumps, variable-speed pumps, etc. To further complicate the situation, different control strategies may be implemented and the operation of the system may be continuous or scheduled. All these factors make it time-consuming to build the system model based on the dynamic system simulation software like TRNSYS, particularly in view of the fact that specific models might be needed for different chiller plant systems to be investigated. Consequently, a more generic modeling approach based on ANN was selected. By using the ANN model, there was no need to consider the detailed operation of the system. Fixed input templates as shown in Appendix A could then be used. The logged data was used to train and test the ANN model. In this regard, the data refinement procedure was crucial in order to build an appropriate system model.

Table 1. Summarized input and output layer of the system model.

Input layer				**Output layer**			
1	T	13	$T_{chwr,2}$	1	Q_e	10	m_{chw}
2	D	14	$T_{chwr,3}$	2	P_{ch}	11	m_{cw}
3	M	15	$T_{chws,2}$	3	P_{chwp}	12	m_{ca}
4	$T_{o,db}$	16	$T_{chws,3}$	4	P_{ct}	13	$T_{chwr,1}$
5	$T_{o,wb}$	17	m_{chw}^{i-1}	5	P_{cwp}	14	$T_{chws,1}$
6	$T_{chwr,1}$	18	$T_{chwr,1}^{i-1}$	6	N_{ch}	15	$T_{chwr,2}$
7	$T_{chws,1}$	19	$T_{chws,1}^{i-1}$	7	N_{chwp}	16	$T_{chwr,3}$
8	T_{cwr}	20	$T_{chwr,2}^{i-1}$	8	N_{ct}	17	$T_{chws,2}$
9	T_{cws}	21	$T_{chws,2}^{i-1}$	9	N_{cwp}	18	$T_{chws,3}$
10	m_{chw}	22	$T_{chwr,3}^{i-1}$				
11	m_{cw}	23	$T_{chws,3}^{i-1}$				
12	m_{ca}						

Before training and testing the system model, it is necessary to define the input and output data sets. The input data set should be taken as much as possible those parameters needed to characterize the system performance. For a dynamic system, the operating parameters in the previous time step can affect the system performance in the current time step. Consequently, it is appropriate to include some of these “old” operating parameters into the input data set. Meanwhile, the output data set mainly highlights the key operating

parameters of those major equipment and the system. Table 1 summarizes the input and output layer of the ANN model used in this study. Here, Inputs 17 to 23 referred to those operating parameters in the previous time step (*i-1*). At maximum three supply and return header streams was considered. As shown in Table 1, only CS were involved for building the system model. There were some parameters that appeared in both the input and output layers. The purpose was to enhance the modeling accuracy of those parameters in the model training process.

The structure of the ANN network can substantially affect the accuracy of the model. In general, the use of more intermediate layers and neurons in each layer can improve the precision of the model but at the expense of longer computation time. While there is no simple way to find the optimal configuration, the usual practice is by repeated trials. In this study, two intermediate layers were employed, the first one having 460 neurons and the second one having 360 neurons. The resulting accuracy of the ANN model was discussed in Section 5. Before conducting the model training, all input and output parameters were normalized between the minimum and maximum values of those parameters in the time-dependent input database. For any input/output parameter *x*, the respective normalized value *X* was given by

$$X = \frac{x - x_{min}}{x_{max} - x_{min}} \quad (1)$$

To train the system modeling, 70% of the time steps in the time-dependent input template (the first part for modeling training and database building) was randomly selected. The remaining was used for model validation (15%) and testing (15%). For a building which is not operating in 24 hours basis, the performance of the chiller system during the night period usually appears to be intermittent which influences the effectiveness of the system modeling. Consequently, in such case, the operating data between 10:00 pm and 8:00 am was not used in system modeling and subsequent sensor fault detection and diagnosis.

2.2.3 Sensor selection

With the ANN model developed, it is necessary to identify which critical sensor signal affects the system performance to a greater extent. This is important as a more

significant difference in the system performance can be detected under the faulty situations for a critical or primary sensor in which the system performance is more sensitive to. To do so, all critical sensors were considered. Again, to facilitate the direct use of the ANN model, normalized parameter values were adopted. For each selected normalized parameter X, a base value (X_{base}) was defined which was taken as the median value in the input database. Then, respective maximum (X_{max}) and minimum (X_{min}) values were found within the input database. The parameter range of X (ΔX) employed in the sensitivity analysis was then determined based on the following approach:

$$\Delta X = Min(X_{max} - X_{base}, X_{base} - X_{min}) \quad (2)$$

$$X_{ll} = X_{base} - sf\Delta X \quad (3)$$

$$X_{ul} = X_{base} + sf\Delta X \quad (4)$$

Here, sf was a span factor which ranged between 0 and 1. The use of this span factor was to ensure that the resulting combination of the operating parameters was within the realistic range. In this study, sf was taken as 0.2.

With the parameter ranges set, respective sensitivity analyses were conducted. The system coefficient of performance (COP_{sys}) was selected as the parameter for comparison. When investigating the system sensitivity to one parameter, base values of the other operating parameters were adopted. The differences in COP_{sys} over the entire parameter range $\{X_{ll}, X_{ul}\}$ in the sensitivity analyses were compared. A greater difference in COP_{sys} indicated a higher sensitivity of the system performance to that parameter.

2.2.4 Sensor fault detection

In SFDet (for database building), the fault pattern database for the fault-free and faulty cases were determined by using the total centroid score (CS_t) as proposed by Luo *et al.* (2009). For each week of the model training dataset, respective fault-free and faulty patterns were generated to characterize the weekly performance of the system by using the modeled results. With N_s selected sensor signals, a normalized fault-free modeled sensor signal dataset $\mathcal{X}_{ff}=\{X_{i,j,ff}, i=1,2,..,t_{max}, j=1,2,..,N_s\}$ was built, where t_{max} was the maximum time step in a week. Then, k-means clustering was applied to group the sensor data into numbers of clusters N where N was given by a rule-of-thumb $N = \sqrt[2]{t_{max}/2}$. With the centroid dataset of the clusters $\mathcal{C}=\{c_{k,j}, k=1,2,..,N, j=1,2,..,N_s\}$ computed, the clustered fault-

free data subsets $\boldsymbol{\mathcal{G}}_{ff}$={$G_{k,ff}$, k=1,N} were determined where $\bigcup_{k=1}^{N}\{G_{k,ff}\} = \boldsymbol{X}_{ff}$. The fault-free total centroid score at any time step ($CS_{t,i,ff}$) was then given by

$$CS_{t,i,ff} = \frac{\|X_{i,ff} - c_k\|}{\left(\frac{\sum_{G_{k,ff}} \|X_{ff} - c_k\|}{n_k}\right)} \quad (5)$$

where n_k is the number of time steps in the clustered subset $G_{k,ff}$ containing that at time step i, and $\|\quad\|$ was the Euclidean distance. Then, all the $CS_{t,i,ff}$ would be divided by the weekly mean fault-free total centroid score [not adopted by Luo *et al.* (2019)] such that

$$CS_{t,i,ff} = \frac{CS_{t,i,ff}}{\left(\frac{\sum_{1}^{t_{max}} CS_{t,i,ff}}{t_{max}}\right)} \quad (6)$$

In SFDet (for evaluation), the weekly centroid score ($CS_{t,i,e}$) profiles based on the modeled results were calculated similarly to those of the fault-free case, i.e.

$$CS_{t,i,e} = \frac{\|X_{i,e} - c_k\|}{\left(\frac{\sum_{G_{k,ff}} \|X_{ff} - c_k\|}{n_k}\right)} \quad (7)$$

and the final values were given by

$$CS_{t,i,e} = \frac{CS_{t,i,e}}{\left(\frac{\sum_{1}^{t_{max}} CS_{t,i,e}}{t_{max}}\right)} \quad (8)$$

In Eq. (7), the same denominator as that used in Eq. (5) on the right hand side was employed. Again, this was different from that proposed in Luo *et al.* (2019) as it was found that a better pattern recognition result could be obtained. Here, the same fault-free cluster centroid dataset was used when evaluating the $CS_{t,i,e}$ and that the weekly fault-free cluster sequence was applied to the weekly evaluation data.

2.2.5 Sensor fault diagnosis

Three types of fault signals were considered in this study, namely bias (B) (both positive and negative), drift (D) (both positive and negative) and precision degradation (P). Each type of fault signal had different characteristics as summarized in Table 2. The instantaneous signal error (e_i) for bias was constant throughout the whole evaluation period while the magnitude increased with time for drift. For precision degradation, it was determined from a Gaussian distribution function ($\boldsymbol{G}$) with mean value zero and standard deviation μ.

Table 2. Summarized characteristics of the different fault signals.

Fault type	Fault strength	Error correlation
Bias	δ	$e_i = \delta$
Drift	ε	$e_i = e_{i-1} + \varepsilon\Delta t$
Precision degradation	μ	$e_i = \boldsymbol{G}(0,\mu)$

To generate the fault pattern database for the faulty cases in SFDia (for database building), a faulty sensor signal was used to determine the faulty system performance through the ANN model where

$$x_{ij,ft} = x_{ij,ff} + e_{ij} \tag{9}$$

Again, normalization of parameters were required when using the ANN model. For each week of data in the modeling training dataset, a faulty total centroid score ($CS_{t,i,ft}$) was defined similar to the evaluation total centroid score in which

$$CS_{t,i,ft} = \frac{\|x_{i,ft} - c_k\|}{\left(\frac{\sum_{G_{k,ff}} \|x_{ff} - c_k\|}{n_k}\right)} \tag{10}$$

Same as that for the fault-free and evaluation total centroid scores, all the $CS_{t,i,ft}$ should be divided by the weekly mean faulty total centroid score as indicated in Eqs. (6) and (8).

Table 3. Definition of different fault cases for both temperature and flow sensors.

Fault type	Strength	Number of cases
Bias	Temperature δ_{min} = 0.1 °C δ_{max} = 1.0 °C Flow δ_{min} = 5% of m_{max} [1] δ_{max} = 10% of m_{max}	10 for positive bias 10 for negative bias
Drift	Temperature ε_{min} = 0.005 °C/h ε_{max} = 0.025 °C/h Flow ε_{min} = 0.1% of m_{max} /h ε_{max} = 1% of m_{max} /h	6 for positive drift 6 for negative drift
Precision degradation	$\mu_{max} = \delta_{max}$ μ_{min} = 10% of μ_{max}	6

1 Maximum system flow.

To build the faulty database, different fault cases were considered. This included all the three fault types with different fault strengths. In this study, two types of sensors were involved, namely temperature and flow sensors. Table 3 summarizes the variation of fault cases investigated. For each sensor signal, there would be totally 38 fault cases. To complicate the situation, if multiple sensor faults were to be dealt with, the number of fault combinations would be enormous (totally 1,520 faulty cases for two sensors only). The required memory and computational time would be very costing. In view of this, a maximum of two sensor signals would be handled in each round of fault evaluation for the critical sensors.

During SFDia (for evaluation), the evaluation profile for each evaluation week would be compared with all the weekly fault-free and faulty profiles week-by-week. The fitness of the profiles was determined by the Euclidean distance between the fault-free/faulty CS_t profiles and the evaluation ones. Then, the fault case with the smallest Euclidean distance would be identified for each evaluation week. The fault case with the highest frequency of occurrence throughout the whole evaluation period would be taken as the fault diagnosis result for the selected critical sensor.

To proceed with the fault evaluation of SS, various **BASE** reference temperatures of CS needed to be established. They were the return chilled water header temperatures and the cooling water supply and return header temperatures (for water-cooled systems only). The chilled water system flow was also necessary if there was no individual chilled water flowmeter for each chiller. To achieve, they had to be checked through the fault evaluation of CS. As mentioned previously, the simultaneous checking of more than two sensors would involve a very large fault pattern database. Hence, it was decided after vigorous trials that the fault evaluation of each return chilled water header temperature would be done together with the system chilled water flow one-by-one. In this regard, the conduction of multiple sensor fault detection, diagnosis and reconstruction could be demonstrated. Then, the fault evaluation of cooling water supply and return header temperatures (if required) would be made individually.

2.2.6 Sensor fault reconstruction

With the fault evaluation of all the critical sensors completed, a reconstruction file would be generated which recorded the starting time (Year, month and day), type ("B" for bias, "D" for drift and "P" for precision degradation) and value of the fault reconstructions. For precision degradation, the reconstruction value was set to zero. For bias and drift, it was simply the negative of the fault value. The information would be used in the fault evaluation of SS to reconstruct the respective CS when appropriate.

2.2.7 Fault evaluation of secondary sensors

As the chiller plant performance was less sensitive to SS, the previous approach of employing pattern recognition technique was not suitable. Instead, the corresponding temperature bias of the SS were computed by using energy and mass balance method. On the chilled water side, the SS included those installed at the chilled water inlet and outlet of each chiller as well as that at the chilled water supply header. On the cooling water side which only applied to water-cooled systems, the SS included those placed at the cooling water inlet and outlet of each chiller as well as the water inlet and outlet of each cooling tower. In actual situations, not all these sensors were available, and the algorithm would check for this.

Before starting the computation of the respective temperature bias profiles, the input dataset were first screened. If the number of installed chillers was greater than two, only those time steps when at least two chillers were in operation would be selected. Otherwise, all those time steps with at least one chiller in operation would be considered. Similar to that in the fault evaluation of CS, only those time steps between 8:00 am to 10:00 pm were considered if the chiller plant was not operated in 24-hours basis.

The algorithm started on the chilled water side. The temperature bias at different locations were determined by using the chilled water return temperature as the **BASE** value. The reference or correct values and the corresponding temperature bias at various locations were determined as follows:

$$T_{ref,chwi,ch} = T_{chwr} \quad (11)$$

Here, the reference value for the chiller entering chilled water temperature ($T_{ref,chwi,ch}$) was taken as the chilled water temperature at the return header. Should there be more than one

chilled water return header, the mean value from all the chilled water return headers was used. Then, the temperature bias of the chilled water temperature sensor at the chiller inlet ($\delta T_{chwi,ch}$) was given by

$$\delta T_{chwi,ch} = T_{chwi,ch} - T_{ref,chwi,ch} \quad (12)$$

The reference temperature ($T_{ref,chwo,ch}$) and the corresponding temperature bias ($\delta T_{chwo,ch}$) of the chilled water temperature sensor at the chiller outlet was calculated from thermodynamics so that

$$T_{ref,chwo,ch} = T_{ref,chwi,ch} - \frac{Q_{ch}}{m_{chw,ch}c_p} \quad (13)$$

$$\delta T_{chwo,ch} = T_{chwo,ch} - T_{ref,chwo,ch} \quad (14)$$

If both chiller *COP* and power input information are available,

$$Q_{ch} = COP_{ch}P_{ch} \quad (15)$$

Otherwise,

$$Q_{ch} = m_{chw,ch}c_p\left(T_{chwi,ch} - T_{chwo,ch}\right) \quad (16)$$

In the latter case, the chilled water temperature bias at both chiller inlet and outlet would be the same, and

$$\delta T_{chwo,ch} = \delta T_{chwi,ch} \quad (17)$$

The reference temperature for the chilled water temperature at the supply header ($T_{ref,chws}$) was computed from energy balance which was given by

$$T_{ref,chws} = \frac{\sum_1^{N_{ch}} m_{chw,ch}T_{ref,chwo,ch}}{\sum_1^{N_{ch}} m_{chw,ch}} \quad (18)$$

The temperature bias at the chilled water supply header (δT_{chws}) was then

$$\delta T_{chws} = T_{chws} - T_{ref,chws} \quad (19)$$

For the cooling water side (only applicable to water-cooled system), the cooling water supply and return temperatures were used as the **BASIS** for calculating the reference temperatures. By applying the similar approach as for the chilled water side, the respective reference temperature and temperature bias at various locations could be calculated as follows:

$$T_{ref,cwi,ch} = T_{cws} \quad (20)$$

$$\delta T_{cwi,ch} = T_{cwi,ch} - T_{ref,cwi,ch} \quad (21)$$

$$T_{ref,cwo,ch} = T_{ref,cwi,ch} + \frac{(Q_{ch}+P_{ch})}{m_{cw,ch}c_p} \quad (22)$$

$$\delta T_{chwo,ch} = T_{chwo,ch} - T_{ref,chwo,ch} \quad (23)$$

$$T_{ref,cwi,ct} = T_{cwr} \quad (24)$$

$$\delta T_{cwi,ct} = T_{cwi,ct} - T_{ref,cwi,ct} \quad (25)$$

$$T_{ref,cwo,ct} = T_{ref,cwi,ct} + \frac{m_{cw}(T_{cwr} - T_{cws})}{N_{ct} m_{cw,ct}} \quad (26)$$

$$\delta T_{cwo,ct} = T_{cwo,ct} - T_{ref,cwo,ct} \quad (27)$$

For each selected time step, the computation of the bias were only made to those sets of equipment which were in operation. Respective trend data of the temperature bias for the SS were then generated. The next step was to smooth or flatten the trend profiles in order to determine the representative bias throughout the whole record period. This was accomplished in three stages. In the first stage, the trend profiles were segmented in various groups by using the moving average approach. A moving average was computed along each trend profile. For a group of temperature bias (δT_m), the moving average before the second instant would be δT_1. The moving average before the third instant would be (δT_1+δT_2)/2, and the corresponding value before the n instant would be given by $\sum_1^{n-1} \delta T_m/(n-1)$. If this value deviated from δT_n by more than 0.3 °C, a new group would be formed starting with δT_n and the new moving average calculated until the end of the trend profile. In the next stage, the trend profile of each group was leveled based on the group average value. The final step involved the merging of adjacent groups with group average values differed by less than 0.2 °C, starting from the first instant of the trend profile. The new average values for the merged groups would then be re-calculated. The process repeated until there was no more group merging. The selection of 0.3 °C in the profile segmentation and 0.2 °C in group merging was based on repeated trials so that the final step averages best represented the original trend profiles.

Upon completion of the calculation, two data files would be created. Appendix C indicates samples of the two files. The first file summarized the checking results of all the sensors including both CS and SS. For CS, it might be bias, drift or precision degradation while it was always bias only for the SS. For air-cooled systems or in case no cooling water flow information was available, only those parameters involving chilled water would be shown. If the usable data set was less than 11 or when no chilled water flow signal was detected, SS checking would not be conducted. Only the results for CS [including the chilled water flow (if flow signal available), chilled water return header temperatures,

cooling water header supply and return header temperatures (for water-cooled system)] would be indicated, and no trend plot would be generated. Depending on the completeness and appropriateness of the dataset, not all the bias of the SS could be determined. Several remark messages might then be shown in the summary file as briefed in Table 4. The second file indicates the temperature bias trend plots (both original and flattened) of all the SS that could be calculated.

Table 4. Summarized remark messages in the overall summary report.

Message	Reason
No signal	This occurred when the collected data values of particular sensor at all the usable time steps were less than 0.1.
Running time insufficient	This occurred when the number of usable time steps of particular chiller or cooling tower was less than 11.
Cannot calculate	This occurred when both the *COP* and power input of the chiller as well as the sensor signal for the chilled water temperature leaving the chiller were unavailable in the calculation of bias for the chilled water temperature leaving the chiller. When this happened, the bias for the chilled water main supply temperature would also be unable to calculate. Moreover, for a water-cooled plant, if the *COP* and cooling capacity of the chiller could not be found, the cooling water temperature leaving the chiller could not be calculated.

It might be queried how the HMSFDDR differentiated between sensor faults and equipment faults. In In a chiller plant, the major types of equipment included chillers, cooling towers for air cooled chillers and water pumps. The failure of these types of equipment could generally be traced from respective fault signals and the readings of correlated secondary sensors. Hence, they could be easily identified by the plant operators through the building automation system. Of course, if equipment faults occurred, the data within the equipment fault period would not be used for the HMSFDDR process. Hence, it could be confident that only sensors faults were found.

3. Algorithm testing procedures

To test the HMSFDDR algorithm, the operating data of four chiller plants were employed. Table 5 summarizes the general information of the four chiller plants. Chiller Plant 1 (CP1) and Chiller Plant 2 (CP2) were water-cooled systems while Chiller Plant 3

(CP3) and Chiller Plant 4 (CP4) were air-cooled ones. Only CP1 was operated in 24-hour basis. The configuration of each chiller plant differed from each other to certain extent.

Table 5. Summarized general information of the four chiller plants.

Item	CP1	CP2	CP3	CP4
Type	Water-cooled	Water-cooled	Air-cooled	Air-cooled
Operation schedule	24 hours	Non 24 hours	Non 24 hours	Non 24 hours
No. of chillers	4	2	4	6
No. of chilled water pumps	4	3	8	6
No. of cooling towers	4	3	NA	NA
No. of cooling water pumps	3	3	NA	NA
Rated plant cooling capacity (kW)	8,440	2,110	3,460	7,345
Rated plant chilled water flow (kg/s)	402	101	228	318
Rated plant cooling water flow (kg/s)	440	119	NA	NA
Design chilled water supply temperature (°C)	7	7	7	7
Design cooling water supply temperature (°C)	30	32	NA	NA
Data time span	2017.07.30 to 2018.08.04	2018.07.29 to 2019.08.03	2019.06.09 to 2020.02.29	2019.06.16 to 2020.02.29
Data time step	15 minutes	15 minutes	5 minutes	5 minutes

Based on the logged plant data, the complete HMSFDDR algorithm was executed for each plant. The modeling accuracies for the various plants would be discussed. The summary results were then compared with those from manual site checking reports to assess the appropriateness of the HMSFDDR algorithm. Here, the judgement was based on whether the HMSFDDR results would bring the same action [reconstruct (if the magnitude of the fault value was greater than 0.5) or not] in the same direction (both positive and negative) as those from the site checking reports for each sensor signal. If yes, the assessment of the HMSFDDR for the respective signal would be declared PASS.

Otherwise, it would be considered FAIL. A HMSFDDR effectiveness ($\zeta_{HMSFDDR}$) was defined in which

$$\zeta_{HMSFDDR} = \frac{Number\ of\ PASS'es}{Number\ of\ sensor\ signals} \times 100\% \quad (28)$$

The reconstruction threshold depended on the accuracy of the sensors used in the plant. It was recommended that the sensor accuracy should not be too low in order to allow a smaller reconstruction threshold to be used.

To further justify the merit of the HMSFDDR, the results from the HMSFDDR were compared with those from off-site testing. Here, particular temperature sensors were collected from various sites and the readings compared with calibrated temperature reading device at various temperature levels. Figure 4 shows the flowchart for the algorithm testing procedure.

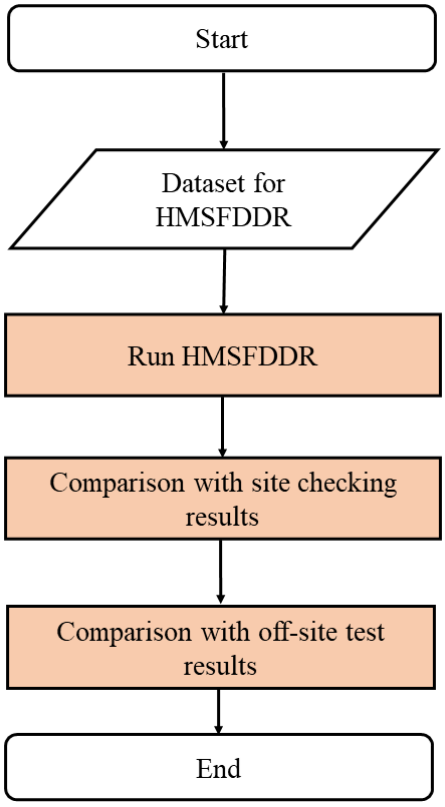

Figure 4. Flowchart for the algorithm testing procedure of the HMSFDDR.

4. Results and discussions

4.1 Analysis of system modeling accuracy

As mentioned in Section 2.2.2, ANN technique was employed to model the chiller system. To investigate the appropriateness of this approach, the respective accuracies of the ANN models for the four chiller plants were analyzed as summarized in Table 6. The wide variation of the calculated model accuracies somehow reflected the quality of the input data. For CP1, no cooling water flow information was provided. Meanwhile, the logged total chilled water flow for CP4 was constant even at mid-night when all the chillers were not in operation. Consequently, the completeness and preciseness of the input data was critical to a proper modeling of the system performance. The data refinement subroutine could only help reset particular out-of-range parameters to their bounded values but not the proper ones. In this regard, it was necessary to ensure that the logged data was appropriate. Otherwise, the reliability of the HMSFDDR results would be affected. For a new system, a new database and system model was needed. Even for the same system, the fault-free database should preferably be updated periodically with a new system model developed in order to cope with the continual change throughout the building life.

Table 6. Summarized accuracies of the ANN model for the four chiller plants.

Plant	Average accuracy
CP1	59.4%
CP2	83.9%
CP3	97.4%
CP4	64.2%

4.2 Summarized HMSFDDR results for the various chiller plants

Table 7 shows the summarized HMSFDDR results for the various chiller plants. The first five rows (those highlighted orange) were CS in which the fault type might be bias, drift or precision degradation. For the four chiller plants considered, there were all found to be bias. When the absolute bias values exceeded 0.5, they were marked with red colors as it meant that reconstruction of the sensor signals were required according to the strategy set in Section 3. For CP1, as no cooling water flow information was available, no calculation could be made for the respective sensors. For CP2, as there were no temperature sensors installed at the cooling water inlet of the cooling towers, no sensor signals were detected and the corresponding fault evaluation could not be made for those sensors.

Table 7. Summarized HMSFDDR results for various chiller plants.

Sensor	Fault (% of maximum flow, °C)			
	CP1	CP2	CP3	CP4
m_{chw}	NF [1]	NF	NF	NF
$T_{chwr,1}$	NF	NF	NF	NF
$T_{chwr,2}$	NF	-0.1 (B)	NA	NA
T_{cwr}	NC [2]	NF	NA	NA
T_{cws}	NC	NF	NA	NA
$T_{chws,1}$	0.19	0.10	-0.58	-1.30
$T_{chws,2}$	0.41	NA	NA	NA
$T_{chwi,Ch1}$	0.18	0.12	0.46	-0.64
$T_{chwo,Ch1}$	-0.04	0.12	0.46	-0.63
$T_{cwi,Ch1}$	NC	0.09	NA	NA
$T_{cwo,Ch1}$	NC	-0.44	NA	NA
$T_{chwi,Ch2}$	-1.94	0.13	-0.46	-0.31
$T_{chwo,Ch2}$	-2.14	0.13	-0.46	-0.31
$T_{cwi,Ch2}$	NC	-0.04	NA	NA
$T_{cwo,Ch2}$	NC	-0.26	NA	NA
$T_{chwi,Ch3}$	0.20	NA	-0.34	-0.62
$T_{chwo,Ch3}$	0.19	NA	-0.34	-0.62
$T_{cwi,Ch3}$	NC	NA	NA	NA
$T_{cwo,Ch3}$	NC	NA	NA	NA
$T_{chwi,Ch4}$	RTI [3]	NA	1.77	-0.80
$T_{chwo,Ch4}$	RTI	NA	1.77	-0.80
$T_{cwi,Ch4}$	NC	NA	NA	NA
$T_{cwo,Ch4}$	NC	NA	NA	NA
$T_{chwi,Ch5}$	NA	NA	NA	-0.6
$T_{chwo,Ch5}$	NA	NA	NA	-0.6
$T_{chwi,Ch6}$	NA	NA	NA	-0.54
$T_{chwo,Ch6}$	NA	NA	NA	-0.54
$T_{cwi,Ct1}$	NC	NS [4]	NA	NA
$T_{cwo,Ct1}$	NC	0.29	NA	NA
$T_{cwi,Ct2}$	NC	NS	NA	NA
$T_{cwo,Ct2}$	NC	0.04	NA	NA
$T_{cwi,Ct3}$	NC	NS	NA	NA
$T_{cwo,Ct3}$	NC	0.11	NA	NA
$T_{cwi,Ct4}$	NC	NA	NA	NA
$T_{cwo,Ct4}$	NC	NA	NA	NA

1 No fault. 2 Not calculated. 3 Running time insufficient. 3 No signal.

Besides CP1, there were no logged *COP* information for the chillers. Hence, the predicted temperature bias for the sensors at chiller inlet and outlet were the same according to Section 2.2.7. The only exception was the chiller water temperature sensors for Chiller 1 in CP4 which exhibited a slight difference. To explain, it was found that during some operating time for Chiller 1, the temperature sensor at the chilled water outlet outputted

some illegal range of data which was ignored by the algorithm. Consequently, the temperature bias profiles for the two chilled water temperature sensors for Chiller 1 were not exactly the same although no *COP* information was provided. For CP2, the predicted sensor faults were weak which did not require reconstruction to be made.

4.3 Comparison of HMSFDDR results with site checking reports

As CP1 had been demolished, no site sensor checking report was available. Hence, the comparison could only be made on CP2, CP3 and CP4. Site checking was the present method used to calibrate the temperature sensors at site. With the system approached a steady state, the temperature sensors (RDT type) were removed from the sensor pockets (one-by-one). At the same time, the measuring probe (also RDT type) of a calibrated temperature reader would be inserted into the sensor pockets. The readings from the temperature sensors (read through the CCMS) were then compared with those from the calibrated temperature reader one-by-one. In site checking, each individual temperature sensor and the measuring probe of the calibrated temperature reader were not placed in the corresponding sensor pocket simultaneously. Tables 8 to 10 summarize the corresponding site sensor checking results (only bias) for the temperature sensors in CP2, CP3 and CP4 respectively together with the HMSFDDR assessment. The assessment result for CP2 was the best with 75% of correct prediction which was then followed by CP3 with 70% HMSFDDR effectiveness. The result for CP4 was the worst in which the HMSFDDR algorithm was only 36% effective. This was not surprising as the model accuracy for CP4 was also the lowest according to Table 6.

Table 8. Site checking results and HMSFDDR assessment for CP2.

Sensor	Fault from site checking report (°C)	HMSFDDR assessment	Sensor	Fault from site checking report (°C)	HMSFDDR assessment
$T_{chwr,1}$	0.3	PASS	$T_{cwo,Ch1}$	-0.1	PASS
$T_{chwr,2}$	-0.1	PASS	$T_{chwi,Ch2}$	-0.2	PASS
T_{cwr}	1.0	FAIL	$T_{chwo,Ch2}$	-0.8	FAIL
T_{cws}	0.1	PASS	$T_{cwi,Ch2}$	-0.3	PASS
T_{chws}	0.1	PASS	$T_{cwo,Ch2}$	-0.5	PASS
$T_{chwi,Ch1}$	-2.4	FAIL	$T_{cwo,CT1}$	-0.2	PASS
$T_{chwo,Ch1}$	-2.3	FAIL	$T_{cwo,CT2}$	-0.1	PASS
$T_{cwi,Ch1}$	-0.4	PASS	$T_{cwo,CT3}$	-0.1	PASS
$\zeta_{HMSFDDR}$					75%

Table 9. Site checking results and HMSFDDR assessment for CP3.

Sensor	Fault from site checking report (°C)	HMSFDDR assessment	Sensor	Fault from site checking report (°C)	HMSFDDR assessment
$T_{chwr,1}$	0.25	PASS	$T_{chwo,Ch2}$	-0.50	PASS
T_{chws}	-1.43	PASS	$T_{chwi,Ch3}$	0.28	PASS
$T_{chwi,Ch1}$	1.80	FAIL	$T_{chwo,Ch3}$	-0.02	PASS
$T_{chwo,Ch1}$	-0.70	FAIL	$T_{chwi,Ch4}$	0.94	PASS
$T_{chwi,Ch2}$	-0.54	FAIL	$T_{chwo,Ch4}$	0.92	PASS
$\zeta_{HMSFDDR}$					70%

Table 10 Site checking results and HMSFDDR assessment for CP4

Sensor	Fault from site checking report (°C)	HMSFDDR assessment	Sensor	Fault from site checking report (°C)	HMSFDDR assessment
$T_{chwr,1}$	0.3	PASS	$T_{chwo,Ch3}$	-0.2	FAIL
T_{chws}	0.3	FAIL	$T_{chwi,Ch4}$	-0.4	FAIL
$T_{chwi,Ch1}$	-0.9	PASS	$T_{chwo,Ch4}$	-0.8	PASS
$T_{chwo,Ch1}$	2.1	FAIL	$T_{chwi,Ch5}$	-0.2	FAIL
$T_{chwi,Ch2}$	-1.8	FAIL	$T_{chwo,Ch5}$	-0.4	FAIL
$T_{chwo,Ch2}$	-3.3	FAIL	$T_{chwi,Ch6}$	-0.1	FAIL
$T_{chwi,Ch3}$	-1.9	PASS	$T_{chwo,Ch6}$	-0.7	PASS
$\zeta_{HMSFDDR}$					36%

It might be expected that the HMSFDDR effectiveness should be the highest for CP3 as the corresponding model accuracy was the best. However, both CP3 and CP4 missed the information for chiller *COP*. Hence, the calculated temperature bias at the chilled water inlet and outlet could only be the same according to Section 3.2.7 as also be found in Table 7. This would somehow restrict the HMSFDDR outcomes and consequently the effectiveness of the algorithm.

4.4 Comparison of HMSFDDR results with off-site testing data

To further justify the accuracy of the HMSFDDR algorithm, off-site tests were conducted for some temperature sensors collected at respective sites. Each temperature sensor was placed in a water pool simultaneously with the measuring probe of the calibrated temperature reader. The readings from the temperature sensors (read through a control module) were then compared with those from the calibrated temperature reader. The sensor readings were compared with a calibrated temperature meter under various water

temperatures. Table 11 summarizes the corresponding off-site test results and the comparison with those from site checking reports and the HMSFDDR algorithm. It could be found that the HMSFDDR algorithm offered results which were closer to those from off-site testing as compared to those from the site checking reports. In this regard, the HMSFDDR algorithm was more reliable than site sensor checking.

Table 11 Comparison of the off-site test results with those from sensor checking reports and HMSFDDR algorithm

Site	Sensor	Temperature bias (°C)			
		Site checking	HMSFDDR	Off-site testing	
				At 17.4 °C	At 20.2 °C
CP2	$T_{chwr,2}$	0.65	0.00	0.28	0.20
CP2	T_{cwr}	0.50	0.30	-0.52	-0.63
CP2	$T_{chwi,Ch1}$	0.40	0.00	-0.18	-0.42
CP5	$T_{chwr,1}$	-0.60	0.54	1.11	0.92

When performing the site sensor checking, the same measuring ports are used for both the sensors and the calibrating device. In this regard, the measurement taken from the sensors and the calibrating device cannot be simultaneous. This can induce some degrees of error particularly for a dynamic system in which the system response can be highly transient. To complicate the situation, substantial time is usually required by the sensors and the calibrating device to obtain steady state results. This further increases the uncertainty in the site checking results. In fact, sensor faults may exhibit some degrees of stochastic nature. Hence, the one-shot site measurement may not truly reflect the actual situation. In this sense, the HMSFDDR effectiveness achieved is considered acceptable, and the proposed new HMSFDDR approach is regarded as an effective method for use in such application. Indeed, this study was supported by one of the major building control suppliers. They provided the required logged data and site checking reports as well as the off-site testing results. Besides the four sites mentioned in the manuscript, they continually apply the algorithm to other sites as they are satisfied with the performance of the algorithm.

5. Conclusions

A hybrid multiple sensor fault detection, diagnosis and reconstruction (HMSFDDR) algorithm for both primary/critical sensors (CS) and secondary sensors (SS) of chiller plants through big data analytics and thermodynamics was developed. It employed ANN

technique to model the chiller plant performance and k-means clustering method to predict various types of sensor faults for CS; while thermodynamics approach to determine the bias for SS. To test the algorithm, logged data from various chiller plants were used and the respective reconstruction results were presented and discussed. Meanwhile, site checking reports were employed to verify the algorithm with the maximum HMSFDDR effectiveness reached 75%. Some key factors that affected the effectiveness of the HMSFDDR algorithm were highlighted. The conduction of off-site sensor testing further reinforced the merit of the HMSFDDR algorithm which deemed the performance of the HMSFDDR algorithm satisfactory.

Nomenclature

Symbols

c	cluster centroid (°C, kg/s)
$\boldsymbol{\mathcal{C}}$	dataset of cluster centroids (°C, kg/s)
COP	coefficient of performance of chiller
COP_{sys}	system coefficient of performance
c_p	specific heat capacity (kJ/kg·°C)
CS_t	total centroid score
D	day of a week
DoM	day of month
e	sensor error (°C, kg/s)
G	clustered data subsets
$\boldsymbol{\mathcal{G}}$	dataset of cluster subsets
$\boldsymbol{G}$	Gaussian distribution function
M	month
m	mass flow rate (kg/s)
$m_{ca,d}$	design air flow rate of cooling tower (m^3/s)
$m_{chw,flag}$	flag for availability of main chilled water flow sensor and signal (1=yes, 0=no)
m_{max}	maximum system mass flow (kg/s)
N	number of clusters
N_{ch}	number of chillers

N_{chwp}	number of chilled water pumps
N_{chrp}	number of chilled water return main pipes
N_{chsp}	number of chilled water supply main pipes
N_{ct}	number of cooling towers
N_{cwp}	number of cooling water pumps
N_s	number of sensor signals
n	number of time steps in each clustered subset
O_{hours}	chiller plant operation schedule ("24 hours", "non-24")
P	power consumption (kW)
P_{name}	chiller plant name
PLF	power limiting factor
Q_{ch}	cooling capacity of individual chiller (kW)
Q_e	system cooling capacity (kW)
sf	span factor
T	temperature (°C)
T_{cooled}	chiller plant type ("air", "water")
$Train_{ratio}$	Training period ratio in the time-dependent input template
t_{step}	time steps per hour
t	time (hour)
t_{max}	maximum time step in a week
x	input/out parameter of system model (°C, kg/s, kW, -)
X	normalized input/output parameter of system model
$\mathcal{X}$	dataset of normalized sensor signals
Y	year
ΔT	temperature change (°C)
δT	temperature bias (°C)
Δt	time step of logged data (hour)
ΔX	span of normalized input/output parameter from the base condition
δ	bias strength (°C, kg/s)
ε	drift strength (°C/hour, kg/s·hour)
μ	standard deviation of Gaussian distribution function (°C, kg/s)
ζ_{MSFDDR}	MSFDDR effectiveness
$\|\ \ \|$	Euclidean distance

Subscripts

1, 2, 3	designation of chilled water supply and return headers
accuracy	accuracy of temperature sensor
base	base condition
ca	cooling tower air
Ch*k*	Chiller *k*
ch	chiller
chw	chilled water
chwi	chilled water at inlet
chwo	chilled water at outlet
chwp	chilled water pump
chwr	chilled water at return header
chws	chilled water at supply header
cw	cooling water
cwi	cooling water at inlet
cwo	cooling water at outlet
cwp	cooling water pump
cwr	cooling water at return header
cws	cooling water at supply header
Ct*k*	Cooling tower *k*
ct	cooling tower
d	design condition
db	dry-bulb
e	evaluation
ff	fault-free
ft	faulty
HMSFDDR	hybrid multiple sensor fault detection, diagnosis and reconstruction
i	designation of time step
j	designation of sensor signal
k	designation of cluster
ll	lower limit
max	maximum
min	minimum

m, n	designation in a temperature bias profile segment
o	outdoor
r	rated value
ref	reference value in MSFDDR of non-critical sensors
set	set point
ul	upper limit
wb	wet-bulb

Superscripts

i-1	previous time step

Abbreviations

AANN	auto-associative neural network
ANN	artificial neural network
B	bias
CP1~4	Chiller Plant 1~4
CS	critical sensors
D	drift
DRef	data refinement
FDD	fault detection and diagnosis
HMSFDDR	hybrid multiple sensor fault detection, diagnosis and reconstruction
NA	not applicable
NC	not calculated
NF	no fault
NS	no signal
P	precision degradation
PCA	principal component analysis
R0..R3	data refinement rule categories
RTI	running time insufficient
SFDD	sensor fault detection and diagnosis
SFDet	sensor fault detection
SFDia	sensor fault diagnosis
SFRec	sensor fault reconstruction
SMod	system modeling

SS	secondary sensors
SSel	sensor selection
SVDD	support vector data description

Disclosure statement

The authors report there are no competing interests to declare.

Funding

The work described in this article was financially supported by Siemens Limited through the Contract Research (Project No. 9231309).

Data availability statement

The participants of this study did not give written consent for their data to be shared publicly, so due to the sensitive nature of the research supporting data is not available.

References

Elnour, M., N. Meskin and M. Al-Naemi. 2020. "Sensor data validation and fault diagnosis using Auto-Associative Neural Network for HVAC systems." *Journal of Building Engineering* 27: 100935.

Gao, L., D. Li, D. Li, L. Yao, L. Liang and Y. Gao. 2019. "A novel chiller sensors fault diagnosis method based on virtual sensors." *Sensors* 19(13): 3013.

Kim, W. and S. Katipamula. 2018. "A review of fault detection and diagnostics methods for building systems." *Science and Technology for the Built Environment* 24(1): 3–21.

Li, G., Y. Hu, H. Chen, H. Li, M. Hu, Y. Guo, S. Shi and W. Hu. 2016. "A sensor fault detection and diagnosis strategy for screw chiller system using support vector data

description-based D-statistic and DV-contribution plots." *Energy and Buildings* 133: 230-245.

Lo, K. K., Leung, S. Y., Zhu, G., Lo, X., Sun, Y., Ngau, Y. C., Leung, K. H., Baek, S. H., Fong, K. F., Lee, C. K. 2022. "A Method and a System of Sensor Fault Management." HK Patent File no. 22021045139.3.

Luo, X. J., K. F. Fong, Y. J. Sun, M. K. H. Leung. 2019. "Development of clustering-based sensor fault detection and diagnosis strategy for chilled water system." *Energy and Building* 186: 17-36.

Ng, K. H., F. W. H. Yik, P. Lee, K. K. Y. Lee and D. C. H. Chan. 2020. "Bayesian method for HVAC plant sensor fault detection and diagnosis." *Energy and Buildings* 228: 110476.

Sun, Y., S. Wang and G. Huang. 2010. "Online sensor fault diagnosis for robust chiller sequencing control." *International Journal of Thermal Sciences* 49(3): 589-602.

Venkatasubramanian, V., R. Rengaswamy, K. Yin and S. N. Kavuri. 2003a. "A review of process fault detection and diagnosis: part I: quantitative model-based methods." *Computer and Chemical Engineering* 27(3): 293–311.

Venkatasubramanian, V., R. Rengaswamy, and S. N. Kavuri. 2003b. "A review of process fault detection and diagnosis: part II: qualitative models and search strategies." *Computer and Chemical Engineering* 27(3): 313–326.

Venkatasubramanian, V., R. Rengaswamy, and S. N. Kavuri. 2003c. "A review of process fault detection and diagnosis: part III: process history based methods." *Computer and Chemical Engineering* 27(3): 327–346.

Wang, S., J. Wang and J. Burnett. 2001. "Validating BMS sensors for chiller condition monitoring." Transactions of the Institute of Measurement and Control 23(4): 201-225.

Wang, S., and J. Cui. 2005. "Sensor-fault detection, diagnosis and estimation for centrifugal chiller systems using principal-component analysis method." *Applied Energy* 82(3): 197-213.

Wang, S., Q. Zhou and F. Xiao. 2010. "A system-level fault detection and diagnosis strategy for HVAC systems involving sensor faults." *Energy and Buildings* 42(2): 477-490.

Wang, S., J. Xing, Z. Jiang and J. Li. 2018. "A decentralized sensor fault detection and self-repair method for HVAC systems." *Building Services Engineering Research and Technology* 39(6): 667-678.

Wu, B., Y. Hu, C. Zhou, G. Chen and G. Li. 2021. “Fault identification for chiller sensor based on partial least square method.” *E3S Web of Conferences* 233: 03057.

Zhang, H., H. Chen, Y. Guo, J. Wang, G. Li and L. Shen. 2019. “Sensor fault detection and diagnosis for a water source heat pump air-conditioning system based on PCA and preprocessed by combined clustering.” *Applied Thermal Engineering* 160: 114098.

Appendix A – Input data templates

A.1 Time-independent input template

Table A.1. Structure of time-independent input template.

Items	Symbol	Default unit	Input
Chiller plant name:	P_{name}	NA	
Type: air/water cooled ("air"/"water")*	T_{cooled}	NA	
Operation schedule ("24 hours"/"non-24") *	O_{hours}	NA	
No. of chillers *	N_{ch}	NA	
No. of chilled water pumps *	N_{chwp}	NA	
No. of cooling water pumps #	N_{cwp}	NA	
No. of cooling towers #	N_{ct}	NA	
Design cooling capacity listed in chiller schedule *	$Q_{e,d}$	kW	
Design chilled water supply temperature listed in chiller schedule *	$T_{chws,d}$	°C	
Design chilled water temperature drop listed in chiller schedule *	$\Delta T_{chw,d}$	°C	
Design chilled water flow rate listed in chiller schedule *	$m_{chw,d}$	kg/s	
Design cooling water flow rate listed in chiller schedule *	$m_{cw,d}$	kg/s	
No. of chilled water supply main pipes (maximum 3) *	N_{chsp}	NA	
No. of chilled water return main pipes(maximum 3) *	N_{chrp}	NA	
Rated power input listed in chilled water pump schedule	$P_{chwp,r}$	kW	
Rated power input listed in cooling water pump schedule	$P_{cwp,r}$	kW	
Maximum cooling water supply temperature listed in cooling tower schedule or flow chart of cooling tower sequence control #	$T_{cws,max}$	°C	
Design cooling water temperature drop listed in cooling tower schedule #	$\Delta T_{cw,d}$	°C	
Design air flow rate listed in cooling tower schedule #	$m_{ca,d}$	m^3/s	
Recorded highest outdoor dry-bulb temperature in Hong Kong's weather observatory history	$T_{o,db,max}$	°C	
Recorded lowest outdoor wet-bulb temperature in Hong Kong's weather observatory history	$T_{o,db,min}$	°C	
Accuracy of temperature sensor (default 0.5)	$T_{accuracy}$	°C	
Time steps per hour (default 4) *	t_{step}	NA	
Rated power input listed in chiller schedule	$P_{ch,r}$	kW	
Rated power input listed in cooling tower schedule	$P_{ct,r}$	kW	
Main chilled water flow sensor installed and log data available (1=yes, 0=no)	$m_{chw,flag}$	NA	
Training period ratio (less than 1.0)	$Train_{ratio}$	NA	

Table A.1 shows the details of the time-independent input template. Those items marked with "*" and "#" are essential parameters but "#" are only applicable to water-cooled systems. It is expected that most of the information required can be found in the equipment schedules of the system.

A.2 Time-dependent input template

Table A.2 indicates the structure of the time-dependent input template. The first 21 columns (A~U) refer to the system operating data. The next 21 columns (V~AP) show the operating data for individual chiller, chilled water pump, cooling water pump and cooling tower. Should there be more than one unit for any type of equipment, additional 21 columns will be added and so on until all equipment units are included. In case the number of units for each type of equipment are not equal, say two sets of chillers with three sets of chilled water pumps, the data for Chiller 3 will be left blank. Again, those items marked with "*" and "#" are essential parameters but "#" are only applicable to water-cooled systems.

Table A.2. Structure of time-dependent input template.

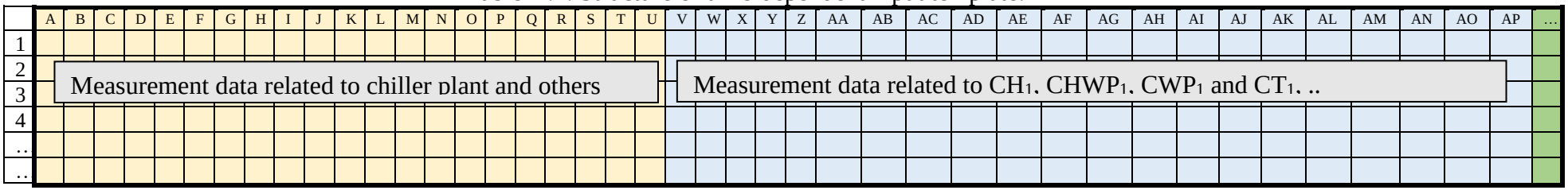

Column	Meaning	Column	Meaning	Column	Meaning	Column	Meaning
A	*Y* (Year)*****	V	P_{ch} of CH_1 (kW) *****	AQ	P_{ch} of CH_2 (kW) *****	…	…
B	*M* (Month)*****	W	On/Off status of CH_1*****	AR	On/Off status of CH_2*****	…	…
C	*DoM* (Day of month)*	X	*COP* of CH_1*****	AS	*COP* of CH_2 (°C) *****	…	…
D	*D* (Day of a week) ***** [1]	Y	$T_{chwi,ch}$ of CH_1 (°C) *****	AT	$T_{chwi,ch}$ of CH_2 (°C) *****	…	…
E	*t* (time) ***** [2]	Z	$T_{chwo,ch}$ of CH_1 (°C) *****	AU	$T_{chwo,ch}$ of CH_2 (°C) *****	…	…
F	T_{chws} at main 1 (°C) *****	AA	m_{chw} of CH_1 (kg/s) *****	AV	m_{chw} of CH_2 (kg/s) *****	…	…
G	T_{chws} at main 2 (°C)	AB	Valve On/Off status of CH_1	AW	Valve On/Off status of CH_2	…	…
H	T_{chws} at main 3 (°C)	AC	$T_{cwi,ch}$ of CH_1 (°C) #	AX	$T_{cwi,ch}$ of CH_2 (°C) #	…	…
I	T_{chwr} at main 1 (°C) *****	AD	$T_{cwo,ch}$ of CH_1 (°C) #	AY	$T_{cwo,ch}$ of CH_2 (°C) #	…	…
J	T_{chwr} at main 2(°C)	AE	m_{cw} of CH_1 (kg/s) #	AW	m_{cw} of CH_2 (kg/s) #	…	…
K	T_{chwr} at main 3 (°C)	AF	P_{chwp} of $CHWP_1$ (kW)	AX	P_{chwp} of $CHWP_2$ (kW)	…	…
L	T_{cws} at main (°C) #	AG	On/Off status of $CHWP_1$	AY	On/Off status of $CHWP_2$	…	…
M	T_{cwr} at main (°C) #	AH	P_{cwp} of CWP_1 (kW)	AZ	P_{cwp} of CWP_2 (kW)	…	…
N	m_{chw} at main (kg/s) *****	AI	On/Off status of CWP_1	BA	On/Off status of CWP_2	…	…
O	m_{cw} at main (kg/s) #	AJ	P_{ct} of CT_1 (kW)	BB	P_{ct} of CT_2 (kW)	…	…
P	$T_{chws,set}$ (°C) *****	AK	On/Off status of CT_1	BC	On/Off status of CT_2	…	…
Q	$T_{cws,set}$ (°C) #	AL	$T_{cwi,ct}$ of CT_1 (°C) #	BD	$T_{cwi,ct}$ of CT_2 (°C) #	…	…
R	Q_e (kW)	AM	$T_{cwo,ct}$ of CT_1 (°C) #	BE	$T_{cwo,ct}$ of CT_2 (°C) #	…	…
S	$T_{o,db}$ (°C) *****	AN	m_{cw} of CT_1 (kg/s) #	BF	m_{cw} of CT_2 (kg/s) #	…	…
T	$T_{o,wb}$ (°C) #	AO	m_{ca} of CT_1 (Hz)	BG	m_{ca} of CT_2 (Hz)	…	…
U	*RH* (%)	AP	Valve On/Off status of CT_1	BH	Valve On/Off status of CT_2	…	…

Remarks: 1. Day of a week: 0 ~ 6 for Sunday ~ Saturday 2. Time: 0, 0.25, 0.5, 0.75, …, 23.0, 23.25, 23.50, 23.75 for 15-minute time step

Appendix B – Data refinement rules

Table B.1. Summarized data refinement rules.

Rule	Description
R0	Conversion of all non-numeric data to numeric.
R1-0	Estimation of all missing data by interpolation.
R1-1	Estimation of missing T_{chwr} (Done in R1-0).
R1-2	Estimation of missing T_{chws} (Done in R1-0).
R1-3	Estimation of missing T_{cwr} (Done in R1-0, not applicable to air-cooled plant).
R1-4	Estimation of missing T_{cws} (Done in R1-0, not applicable to air-cooled plant).
R1-5	Estimation of missing $T_{o,db}$ (Done in R1-0).
R1-6	Estimation of missing $T_{o,wb}$ (Done in R1-0, not applicable to air cooled plant).
R1-7	Estimation of missing m_{chw} when all missing. *If $m_{chw} = 0$, set $m_{chw} = \sum_1^{N_{ch}} m_{chw,ch}$.*
R1-8	Estimation of N_{ch} when all missing. *If $P_{ch} > PLF$ [1] $* P_{ch,r}$, set $P_{ch} = PLF * P_{ch,r}$.* *If $P_{ch} > 0.1 * P_{ch,r}$, chiller is on. Otherwise, chiller is off.*
R1-9	Estimation of N_{chwp} when all missing. *If $P_{chwp} > PLF * P_{chwp,r}$, set $P_{chwp} = PLF * P_{chwp,r}$.* *If $P_{chwp} > 0.1 * P_{chwp,r}$, chilled water pump is on. Otherwise, chilled water pump is off.*
R1-10	Estimation of N_{ct} when all missing (Not applicable to air-cooled plant). *If $P_{ct} > PLF * P_{ct,r}$, set $P_{ct} = PLF * P_{ct,r}$.* *If $P_{ct} > 0.1 * P_{ct,r}$, cooling tower is on. Otherwise, cooling tower is off.*
R1-11	Estimation of N_{cwp} when all missing (Not applicable to air-cooled plant). *If $P_{cwp} > PLF * P_{cwp,r}$, set $P_{cwp} = PLF * P_{cwp,r}$.* *If $P_{cwp} > 0.1 * P_{cwp,r}$, cooling water pump is on. Otherwise, cooling water pump is off.*
R1-12	Estimation of m_{cw} when all missing (Not applicable to air-cooled plant). *If $m_{cw} = 0$, set $m_{cw} = \sum_1^{N_{ch}} m_{cw,ch}$.*
R2-1	Check if $T_{o,db}$ exceeds upper limit. *If yes, reset value to upper limit.*
R2-2	Check if $T_{o,db}$ below lower limit. *If yes, reset value to lower limit.*
R2-3	Check if $T_{o,wb}$ exceeds $T_{o,db}$. *If yes, reset value to dry-bulb temperature.*
R2-4	Check if T_{chws} below lower limit. *If yes, reset value to chilled water supply setpoint.*
R2-5	Check if ΔT_{chw} exceeds upper or lower limit (Not applicable to multiple chilled and return headers as well as evaluation data). *If $\Delta T_{chw} > \Delta T_{chw,d}$, set $T_{chwr} = T_{chws} + \Delta T_{chw,d}$.* *If $\Delta T_{chw} < 0$, set $T_{chwr} = T_{chws}$.*
R2-6	Check if T_{cws} exceeds upper limit (Not applicable to air-cooled plant). *If less than 5% of data exceeds limit, reset value to cooling water supply setpoint. Otherwise, no refinement.*

1 *PLF* is a power limiting factor which is currently set to 2.

Table B.1. Summarized data refinement rules (continued).

Rule	Description
R2-7	Check if ΔT_{cw} exceeds upper or lower limit (Not applicable to air-cooled plant). *If* $\Delta T_{cw} > \Delta T_{cw,d}$, *set* $T_{cwr} = T_{cws} + \Delta T_{cw,d}$. *If* $\Delta T_{cw} < 0$, *set* $T_{cwr} = T_{cws}$.
R3-1	Check and refine chilled water system data conflict against N_{ch} and N_{chwp}. *If* $(T_{chwr} < T_{chws})$ *AND* $(N_{chwp} = 0)$ *AND* $(N_{ch} /= 0)$, *set* $N_{ch} = 0$. *If* $(T_{chwr} < T_{chws})$ *AND* $(N_{chwp} /= 0)$ *AND* $(N_{ch} /= 0)$, *set* $T_{chws} = T_{chws,set}$.
R3-2	Check and refine cooling water system data conflict against N_{ch} and N_{ct} (Not applicable to air cooled plant). *If* $(T_{cwr} < T_{cws})$ *AND* $(N_{ct} = 0)$ *AND* $(N_{ch} /= 0)$, *set* $N_{ch} = 0$. *If* $(T_{cwr} < T_{cws})$ *AND* $(N_{ct} /= 0)$ *AND* $(N_{ch} /= 0)$, *set* $T_{cws} = T_{cws,set}$.
R3-3	Check and refine chilled water pump operating data conflict. *If* $(m_{chw} = 0)$ *AND* $(P_{chwp} = 0)$ *AND* $(N_{chwp} /= 0)$, *set* $N_{chwp} = 0$. *If* $(m_{chw} = 0)$ *AND* $(P_{chwp} > 0)$ *AND* $(N_{chwp} /= 0)$, $m_{chw} = m_{chw,d} * Q_e / (N_{ch} * Q_{ch,d})$.
R3-4	Check and refine cooling tower operating data conflict (Not applicable to air-cooled plant). *If* $(T_{cwr} < T_{cws})$ *AND* $(m_{ca} = 0)$ *AND* $(N_{ct} /= 0)$, *set* $N_{ct} = 0$. *If* $(T_{cwr} < T_{cws})$ *AND* $(m_{ca} /= 0)$ *AND* $(N_{ct} /= 0)$, $T_{cws} = T_{cws,set}$ $T_{cwr} = T_{cws} + (Q_e + P_{ch}) / (m_{cw} * c_p)$. *If* $(T_{cwr} < T_{cws})$ *AND* $(m_{ca} /= 0)$ *AND* $(N_{ct} = 0)$, *set* $m_{ca} = 0$.
R3-5	Check and refine cooling water pump operating data conflict (Not applicable to air-cooled plant). *If* $(m_{cw} = 0)$ *AND* $(P_{cwp} = 0)$ *AND* $(N_{cwp} /= 0)$, *set* $N_{cwp} = 0$.
R3-6	Check and refine N_{ch} against N_{ct}, N_{chwp} and N_{cwp} (Not applicable to air-cooled plant). *If* $(N_{ch} /= 0)$ *AND* $(N_{chwp} = 0)$ *AND* $(N_{ct} = 0)$, *set* $N_{ch} = 0$. *If* $(N_{ch} /= 0)$ *AND* $(N_{cwp} = 0)$ *AND* $(N_{ct} = 0)$, *set* $N_{ch} = 0$. *If* $(N_{ch} /= 0)$ *AND* $(N_{chwp} = 0)$ *AND* $(N_{cwp} = 0)$, *set* $N_{ch} = 0$.
R3-7	Check and refine N_{chwp} against N_{ch}. *If* $(N_{chwp} = 0)$ *AND* $(N_{ch} /= 0)$, *set* $N_{chwp} = N_{ch}$.
R3-8	Check and refine N_{ct} against N_{ch} (Not applicable to air-cooled plant). *If* $(N_{ct} = 0)$ *AND* $(N_{ch} /= 0)$, *set* $N_{ct} = N_{ch}$.
R3-9	Check and refine N_{cwp} against N_{ct} (Not applicable to air-cooled plant). *If* $(N_{cwp} = 0)$ *AND* $(N_{ct} /= 0)$, *set* $N_{cwp} = N_{ct}$.

Appendix C – Sample of overall sensor checking reports

A sample of the sensor checking summary report is given below. Figure C.1 shows samples of the temperature bias trend plots for non-critical sensors. The orange lines represent the flattened profiles while the blue lines are the original ones.

Chiller plant sensor fault checking report...

Total number of raw data set = 35616
Total number of usable data set = 17789

Maximum system chilled water flow = 100.8 kg/s

Sensor	Fault type	Value	
m_chw		No fault	
T_chwr_1		No fault	
T_chwr_2	Bias	-0.10	degC
T_cwr		No fault	
T_cws	Bias	-0.10	degC
T_chws	Bias	0.10	degC
T_chwi_Ch1	Bias	0.02	degC
T_chwo_Ch1	Bias	0.02	degC
T_cwi_Ch1	Bias	0.08	degC
T_cwo_Ch1	Bias	-0.44	degC
T_chwi_Ch2	Bias	0.13	degC
T_chwo_Ch2	Bias	0.13	degC
T_cwi_Ch2	Bias	-0.04	degC
T_cwo_Ch2	Bias	-0.25	degC
T_cwi_CT1		No signal	
T_cwo_CT1	Bias	0.29	degC
T_cwi_CT2		No signal	
T_cwo_CT2	Bias	0.04	degC
T_cwi_CT3		No signal	
T_cwo_CT3	Bias	0.11	degC

Sensor fault checking completed...

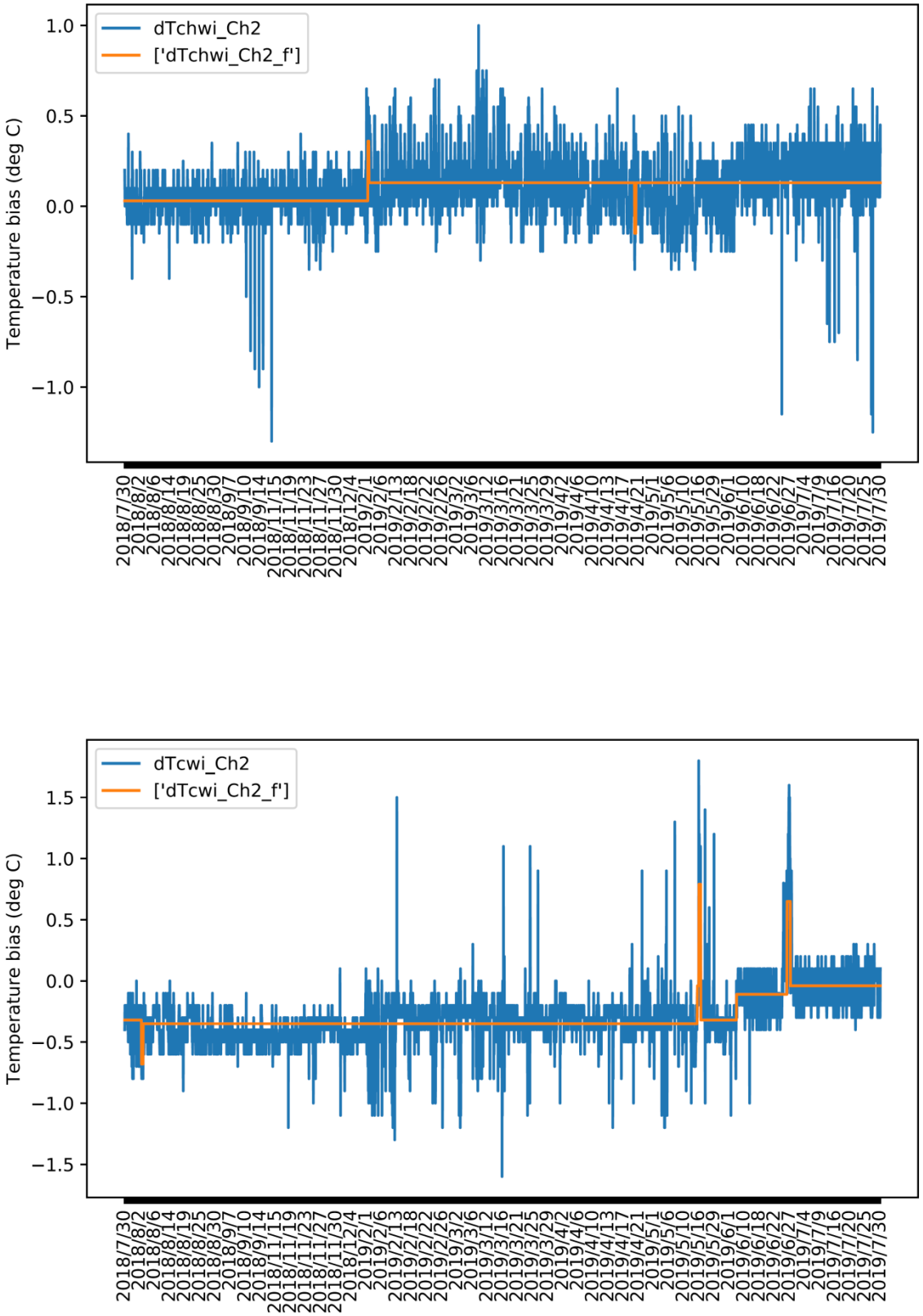

Figure C.1. Samples of temperature bias trend plots for secondary sensors.